



Flow through nets and trawls of low porosity

Svein Helge Gjørund*, Birger Enerhaug

SINTEF Fisheries and Aquaculture, Fisheries Technology, NO-7465 Trondheim, Norway

ARTICLE INFO

Article history:

Received 21 April 2009

Accepted 7 January 2010

Available online 13 January 2010

Keywords:

Fisheries

Trawl

Plankton nets

Flow

Filtration efficiency

Drag

Pressure drop

ABSTRACT

In trawls intended for harvesting marine zooplankton the mesh size and twine thickness may be as small as $O(10^{-4} \text{ m})$, the porosity less than 0.5 and the appropriate Reynolds number $O(10^0 - 10^2)$. The flow locally through the meshes varies strongly with the Reynolds number in this range, and the entire flow field, filtered volume and drag of such nets therefore depend strongly on the net parameters and towing velocity.

This paper presents a simplified model for the flow through and forces on inclined permeable screens based on pressure drop considerations. For conical nets the model provides simple expressions for the filtration efficiency and drag as functions of twine diameter, mesh opening, porosity, taper angle and flow (towing) velocity. Comparisons with test tank measurements of typical plankton nets show good agreement.

© 2009 Elsevier Ltd. All rights reserved.

1. Introduction

Limited commercial fishing for red feed (*Calanus finmarchicus*) is currently being developed in Norway, and in recent years there has been an increase in international fishing for Antarctic krill (*Euphausia superba*) in the Southern Ocean. A *Calanus finmarchicus* individual is typically 0.5 mm thick and 2–3 mm long when it is harvested, while an Antarctic krill is roughly 10 times bigger. Other small zooplankton may also attract commercial interest in the future. The fishing gear used to catch these species is fine-meshed trawls, having low taper angles and large filtering net areas and being towed at low velocities, typically at 0.5 m/s. Except for empirical relations for the filtration performance and clogging rate of small net samplers used in oceanographic research, no satisfactory model for the flow through such nets exists. In future harvesting of zooplankton by means of trawls it will be important to optimize catch and fuel efficiency and catch quality; hence improved hydrodynamic models are needed.

The flow through the main part of traditional fish trawls is usually considered uniform and undisturbed by the trawl. The porosity of such trawls is relatively high, typically $\beta > 0.8$, and the Reynolds number based on twine diameter Re_d is of the order $O(10^3 - 10^4)$. The drag forces are approximated by summing the drag on the individual twines and knots, using the cross-flow principle for undisturbed flow (towing) velocity and suitable drag coefficients. Several authors indicate that this approach is

permissible for $\beta \geq 0.7$, depending also on other net parameters (Hoerner, 1952, 1965; Koritzky, 1974; Paschen and Winkel, 1999; Fredheim, 2005). A model for the flow through trawls of high and intermediate porosities is developed by Fredheim (2005), modeling the twines and knots as line and point sources, respectively, and invoking a velocity defect model for the wakes of the individual twines. Fredheim (2005) states that compared with net panels and net cages, changes in the geometry of a given net cone do not seem to have a large influence on the drag force on the cone, and that the relative pressure variations in front of and inside a trawl are small. The geometry and towing resistance of trawls are often studied in model tests. Different scaling methodologies and empirical corrections exist for the building of the model scale trawl and for the scaling of velocities and forces, but Reynolds scaling is seldom possible and Reynolds number effects are usually neglected (see e.g. Fridman and Carrothers, 1986; Ward and Ferro, 1993; O'Neill, 1993; Ferro et al., 1996; Hu et al., 1999).

In trawls intended for *Calanus finmarchicus* the mesh size and twine thickness will both be of the order $O(10^{-4} \text{ m})$, the porosity $\beta \approx 0.5$ and $Re_d = O(10^0 - 10^2)$. The boundary layer outside the twines, i.e. the region of viscous displacement and reduced velocity, generally increases in thickness with decreasing Reynolds number. For high Reynolds number the boundary layer is very thin compared with the twine diameter, while for very low Reynolds numbers the region of viscous displacement may extend several diameters outside the twine. Due to the low taper angle the normal velocity component just in front of the net wall may be very low and combined with the very thin twines in such netting, the resulting Reynolds number Re_d becomes very low. Due to the close spacing between the twines, the entire flow field,

* Corresponding author. Tel.: +47 91132735.

E-mail address: Svein.H.Gjorund@sintef.no (S.H. Gjørund).

Symbols			
A_0	projected screen area in the direction of U ; for a trawl/net cone A_0 equals the mouth area	Re_d	Reynolds number based on twine diameter
A_{screen}	total screen (net) area	Re_D	Reynolds number based on mouth diameter
C_D	overall drag coefficient in the direction of U , normalized by U and A_0	T_γ	tangential stress coefficient due to streamline deflection across screen
C_L	overall lift coefficient in the direction transverse to U , normalized by U and A_0	T_f	tangential stress coefficient due to friction along screen
C_N	normal force coefficient due to pressure drop K , normalized by U and A_{screen}	u_0	the average velocity component in the direction of U of the flow that passes through the screen; for a trawl/net cone u_0 equals the average velocity across the mouth
d	twine diameter	u_1	normal velocity component just in front of the screen
D	source parameter in Koo and James (1973)	U	undisturbed flow (towing) velocity some distance upstream of the screen (net)
F	filtration efficiency; $F=u_0/U$	α	taper angle
F_D	drag force	β	porosity; for square meshes $\beta=m^2/(d+m)^2$
F_L	lift force	γ	the angle the flow leaving the screen makes to the normal to the screen
K	pressure drop coefficient	Δ	parameter in Gibbins (1973)
K_0	pressure drop coefficient for $\alpha=90^\circ$	λ	the ratio of the channel height filled by the screen in Koo and James (1973)
m	mesh bar length	ν	kinematic viscosity
Δp	pressure drop	ρ	density
r	radial coordinate	τ	tangential stress
R	radius of net mouth		
R_A	ratio between open-mesh area and mouth area of a net; for a net cone of constant taper ratio and porosity $R_A = \beta A_{screen}/A_0 = \beta/\sin\alpha$		

filtered volume and drag of such nets therefore depend strongly on the net parameters and towing velocity.

The flow through three-dimensional nets is complex and difficult to model both theoretically and numerically. The purpose of the present work is to provide a simplified parametric model for such flow, so that the effect of varying mesh size, twine thickness, taper angle and other net parameters can be estimated in a relatively simple manner, and to provide a theoretical basis for correct scaling of such nets in model tests. A limited review of the literature on the filtration efficiency of zooplankton net samplers is given, along with a summary of basic results for the pressure drop across permeable screens. The latter are then used to derive a simplified model for the flow through inclined permeable screens. For trawls or net sections of general geometry the resulting equations must be integrated over the net area. For the simple case of a conical net of circular cross-section and constant taper angle and mesh parameters, however, the expressions for the overall filtration efficiency and drag follow directly from those for an inclined screen. Finally, model predictions are compared with measurements for conical nets made out of typical plankton netting.

2. Filtration efficiency of zooplankton net samplers

Zooplankton collecting systems are described in Wiebe and Benfield (2003) and Harris et al. (2000). A much-used design parameter for plankton nets is the “open-mesh-filtering-area to mouth area ratio” R_A . Tranter and Smith (1968) find that the filtration efficiency F increases with R_A for $R_A < 3$, while it tends to flatten out for $R_A > 3$. Harris et al. (2000) recommend that R_A be at least 6 for horizontally towed nets to have a buffer against clogging of meshes.

Smith et al. (1968) test a series of cylindrical, conical and cylindrical–conical nets (cylindrical forepart, conical aft) in the range $3.2 < R_A < 6.4$, in addition to one cylindrical net with $R_A=1.6$. The mouth diameter is 1 m and the towing velocity 1.13 m/s for all cases, and F is taken as the ratio between an

assumedly representative velocity measured inside the net mouth and one measured outside. The velocity inside the mouth is measured at a distance of $0.7 R \approx \sqrt{2}/2R$ from the centre of the mouth, i.e. at the radial centre of gravity of the mouth area, cf. Fig. 1. This yields a better estimate of the average velocity across the mouth than the velocity measured at the very centre. Smith et al. (1968) find that the initial filtration efficiency is 85–95% for all but one of the nets, the net with $R_A=1.6$ having an initial filtration efficiency of only 71%. This shows that high initial filtration efficiency can be ensured by proper design, and Smith et al. (1968) and Tranter and Smith (1968) emphasize the sustained (i.e. after clogging occurs) filtration efficiency as the main concern for plankton nets. Smith et al. (1968) present empirical formulas for estimating the minimum R_A necessary for keeping clogging at a satisfactorily low level in waters of different clarity. They find that the cylindrical and cylindrical–conical nets have higher sustained filtration efficiency than the purely conical nets, and attribute this to oscillations in the netting which are more pronounced in the cylindrical sections. They suggest that such oscillation can be promoted by designing the net with a low pressure difference across the net wall (i.e. a low pressure drop), or by reducing the tension in the netting by means of longitudinal support webbing (i.e. causing a slack). They further state that the cylindrical nets were difficult to tow and recover, and therefore generally recommend cylindrical–conical nets.

Tranter and Heron (1967) test net samplers with mouth diameters 0.12–0.57 m, and make measurements and observations

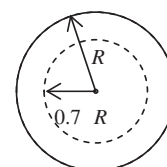


Fig. 1. Circular net mouth with radius R . The area inside the dashed line equals half the mouth area. Smith et al. (1968) measure the assumedly representative mouth velocity at the dotted line ($r=0.7R$) instead of at the mouth center ($r=0$).

of the filtration efficiency and the flow pattern through and around the samplers. The nets in these tests are conical and have a flare attached in the front, i.e. an expanding solid (fiberglass) cone in front of the net, cf. Fig. 2c. Tranter and Heron (1967) and Tranter and Smith (1968) present visualizations of the flow pattern through samplers with and without flares. In flow through and around an expanding cone in a free flow, there will be an increased velocity outside the outlet of the cone, and consequently a reduced pressure across the outlet which tends to cause a suction of the flow through the smaller inlet. For an appropriately designed flare this yields a higher and more uniform velocity across the inlet of the flare than there would be across the mouth of the conical net alone. The mean velocity across the inlet of the flare may approach the towing velocity, and it is also reported to exceed the towing velocity in some cases. In the literature on zooplankton net samplers, flares are thus said to increase the filtration efficiency. However, it must be noted that the filtration efficiency is then determined with respect to the smaller inlet area of the flare and not with respect to the larger mouth area of the filtering net. Hence, higher filtration efficiency for a flared net does not necessarily imply an increased flow or filtered volume compared with an identical net without flare. However, it is assumed that the more uniform flow through the mouth of the flare prevents zooplankton from avoiding the sampler and that flared samplers provide biologically less biased samples. Also, flared samplers are better suited for high towing velocities. Tranter and Heron (1967) find that the effectiveness of the flares is inversely proportional to the angle of expansion of the flare (it is indicated that angles less than 3.5° are appropriate) and proportional to its length. However, they also find that samplers with flare clog more readily in field experiments than the samplers without flare. Flares of canvas were also tested but showed a tendency to collapse. Tranter and Heron (1967) state that “contrary to common belief” the filtration efficiency of both coarse and fine nets decreases with decreasing velocity, in particular for towing velocities less than 0.50 m/s.

Tranter (1967) proposes a formula for the filtration of plankton nets, based on Taylor and Davies (1944) and introducing an additional empirical constant. However, the model of Taylor and Davies (1944) applies to a porous plane screen perpendicular to an incident flow and it is not directly applicable to a three-dimensional net. The experimental procedure and quantities in Tranter (1967) are unclear, i.e. there is no clear distinction between the pressure drop coefficient and the drag coefficient. Hence, the formula does not appear to have sufficient theoretical basis or to be convincingly verified by experiments.

3. Pressure drop across a permeable screen

Existing literature on flow through permeable screens mainly considers plane or slightly curved screens that are normal to or close to normal to an incident flow and fill the entire or greater part of a channel. The primary application is flow control in test tanks and wind tunnels, and the solutions are not directly applicable to three-dimensional net structures. A permeable screen affects an incident flow in two ways: by a reduction in the static pressure across the screen and by a deflection of the streamlines towards the normal to

the screen, cf. Fig. 3. The netting in trawls generally has a small angle of incidence α to the flow (towing) direction. The screen angle of incidence is therefore here defined such that $\alpha=0^\circ$ for a screen parallel to the flow, $\alpha=90^\circ$ for a screen normal to the flow and $(\pi/2-\alpha)$ is the angle the incident flow makes to the normal to the screen. The angle the flow leaving the screen makes to the normal is $\gamma \leq (\pi/2-\alpha)$. For low porosities, i.e. $\beta < 0.5$, the flow will approach and pass more or less normally through the screen (Reynolds, 1969), while for higher porosities the deflection towards the normal to the screen becomes gradually weaker. For a screen that does not fill the entire cross-section of a channel, the flow will to some extent be blocked by and deflected around it. It is therefore useful to define three velocities: U —the undisturbed flow (towing) velocity some distance upstream of the screen, u_0 —the average velocity component in the direction of U of the flow that actually passes through the screen, and u_1 —the normal velocity component just in front of the screen. The relation between these three velocities is $u_1 = u_0 \sin \alpha \leq U \sin \alpha$.

The pressure drop coefficient K for a permeable screen is defined by Eq. (2), and K_0 is defined as $K_0 = K(\alpha=90^\circ)$. For a plane screen normal to the incident flow Eq. (3) applies, where $C_D = C_N$ is the overall drag coefficient for the screen normalized by the free flow velocity. A number of models for K_0 have been proposed, e.g. Hoerner (1952), Wieghardt (1953), Carrothers and Baines (1975), Laws and Livesey (1978), Brundrett (1993) and Wakeland and Keolian (2003). Here we only include the model of Brundrett (1993), since it is based on several of the earlier models and empirical results and covers a wide Re_d -range. Brundrett (1993) verifies the model against measurements of Schubauer et al. (1950) for screens with porosities $0.2 < \beta < 0.8$, and Groth and Johansson (1988) for screens with porosities $0.6 < \beta < 0.7$. K_0 generally increases with decreasing Reynolds number and decreasing porosity. For very low Reynolds numbers viscosity dominates and $K_0 \sim 1/Re_d$. For high Reynolds numbers the Reynolds number dependency vanishes and K_0 can be approximated by a function of the porosity only. For inclined screens ($0^\circ < \alpha < 90^\circ$) Schubauer et al. (1950) demonstrate that Eq. (5) describes the pressure drop well for $\alpha \geq 45^\circ$. Carrothers and Baines (1975) find that measured K for $\alpha < 45^\circ$ exceeds that predicted by Eq. (5). However, as pointed out by O'Neill (1993), their model applies to high Reynolds numbers only and therefore fails to account for the strong increase in K_0 as $Re_d(u_1 = u_0 \sin \alpha)$ drops below $O(10^2)$. Hence we here assume that Eq. (5) is applicable for small values of α also, given that the Reynolds number dependency of K_0 is properly accounted for. Deflection of streamlines implies a tangential stress T_γ due to change of

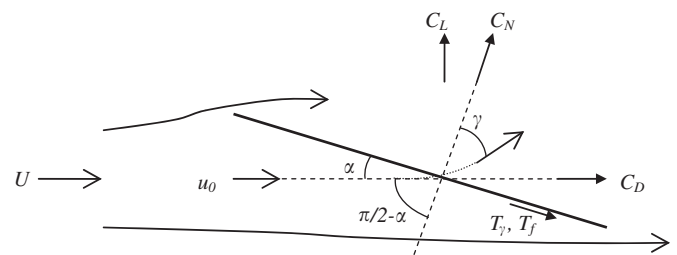


Fig. 3. Sketch of flow through and around an inclined permeable screen.

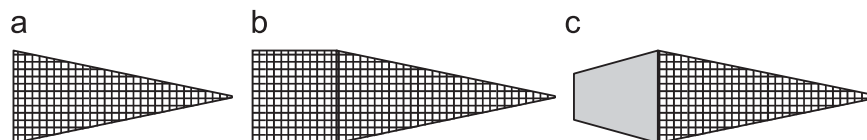


Fig. 2. Idealized net sampler geometries: conical (a), cylindrical-conical (b) and flared (c). Cod-end details left out.

momentum, as given by Eq. (6) (Taylor and Batchelor, 1949). For γ the best available model appears to be that of Gibbings (1973) (see also Laws and Livesey, 1978), cf. Eq. (7). Gibbings (1973) demonstrates that his model compares well with the measurements by Dryden and Schubauer (appendix to Taylor and Batchelor, 1949), which lie in the range $K_0 < 5-6$ for $\alpha \geq 45^\circ$ and $Re_d < O(100)$. As for Eq. (5) we here assume that Gibbings' model applies for lower angles of incidence also, but ideally a verification of the model beyond the given range or a more general model should be sought.

The models for K_0 and K are basically independent of mesh geometry, i.e. they are not derived for one particular mesh type only. Still, the measurements that pressure drop models are correlated with usually pertain to square meshes, so some variation may be expected for other mesh geometries. Variations and imperfections in twine diameters and porosity may also have a significant effect. Brundrett (1993) provides an approximate expression for the error due to variations in twine diameter, and suggests that it can be used as an approximation for all screen dimensional errors and dirt build-up (e.g. marine growth or clogging). The expression for T_γ in Eq. (6) is derived from basic momentum considerations and has general validity, but it requires that the deflection is known. When deriving the expression for the deflection γ , however, Gibbings (1973) assumes that only twines parallel to the axis of deflection contribute, hence Gibbings's model has more limited validity and accuracy.

Several models exist also for the normal force coefficient C_N as a function of pressure drop (see Koo and James, 1973; Løland, 1991; O'Neill, 2006). Such models originate in the source model of Taylor (1944) and Taylor and Davies (1944), but in their original model C_N decreases as K exceeds 4 and vanishes for $K \rightarrow \infty$ (Graham, 1976). Following the same basic approach, but arguing that the source strength is related to the free flow velocity U rather than u_1 , Løland (1991, 1993) derives Eq. (8) for two-dimensional flow past a plane screen requiring that $C_N \rightarrow 2$ as $K \rightarrow \infty$, i.e. the commonly accepted drag coefficient for a solid plate in two-dimensional flow (Hoerner, 1965). Løland (1993) finds that his model compares well with measurements presented in Graham (1976) for values of K up to 10^2 . Koo and James (1973) propose Eq. (9) for two-dimensional flow, where λ is the ratio of the channel height filled by the screen and D is an implicitly given source parameter. Their model yields $C_N \rightarrow 1$ for a solid plate in infinite flow ($\lambda=0$), hence comparing better to three-dimensional flow since the drag coefficient for a solid circular disk or square plate is 1.2, also for values of K up to 10^2 (Graham, 1976). Løland (1991) demonstrates that his model gives comparable results to Koo and James's for $K < 10$ when $\lambda=0$ and for $K < 10^2$ when $\lambda \approx 0.15$.

Combining Eqs. (4) and (8) or (9) in Eq. (3) now yields an estimate of the filtration efficiency of a plane permeable screen normal to a uniform incident flow.

$$Re_d = \frac{u_1 d}{\nu} \quad (1)$$

$$K = \frac{\Delta p}{(1/2)\rho u_1^2} \quad (2)$$

$$\frac{1}{2} C_D U^2 = \frac{1}{2} K_0 u_1^2 \rightarrow \frac{u_1}{U} = \sqrt{\frac{C_D}{K_0}}, \quad \alpha = 90^\circ, \quad C_D = C_N \quad (3)$$

$$K_{0,Brundrett} \approx \left[\frac{7.0}{Re_d} + \frac{0.9}{\log(Re_d + 1.25)} + 0.05 \log(Re_d) \right] \frac{1 - \beta^2}{\beta^2}, \quad 10^{-4} < Re_d < 10^4 \quad (4)$$

$$K(\alpha) = K_0 (u_1 = u_0 \sin \alpha) \sin^2 \alpha \quad (5)$$

$$T_\gamma(\alpha) = \frac{\tau}{(1/2)\rho u_0^2} = 2 \sin^2 \alpha \left[\tan\left(\frac{\pi}{2} - \alpha\right) - \tan \gamma \right], \quad 0 < \gamma < \frac{\pi}{2} - \alpha \quad (6)$$

$$\gamma_{Gibbings} = \tan^{-1} \left[\Delta \tan\left(\frac{\pi}{2} - \alpha\right) \right], \quad \Delta = \left[\left(\frac{K_0}{4}\right)^2 + 1 \right]^{1/2} - \frac{K_0}{4}, \quad 0 < \gamma \leq \frac{\pi}{2} - \alpha \quad (7)$$

$$C_{N,Løland} = \frac{2}{K} [K + 1 - \sqrt{2K + 1}] \quad (8)$$

$$C_{N,Koo \& James} = \frac{K}{(1 + \frac{1}{2} DK)^2 \left[1 - \frac{\lambda DK}{2 + DK} \right]^2}, \quad K = \frac{2DK + (DK)^2}{(1 + DK)^2} \left[2 + \frac{DK}{2}(1 + \lambda) \right]^2 \quad (9)$$

4. A simplified model for the flow through inclined screens

In Eq. (3) the filtration efficiency for a plane screen normal to the incident flow is expressed as a relationship between the force coefficients associated with U and u_0 , respectively. In order to establish a corresponding relation for an inclined screen we do the same, but include the tangential forces and force coefficients also. This means that we establish two equivalent expressions for the drag force on the screen: one using force coefficients associated with u_0 and one using force coefficients associated with U . It is assumed that filtration is evenly distributed over the screen area. Separation from outer edges and global wake effects are neglected.

It is useful to relate the force coefficients to the projected area of the screen in the direction of the incident flow. The relationship between the total screen area A_{screen} and the projected area A_0 for an inclined plane screen is given by

$$\frac{A_{screen}}{A_0} = \frac{1}{\sin \alpha} \quad (10)$$

The force coefficients associated with u_0 are K for the force normal to the screen and T_γ for the force parallel to the screen, cf. Eqs. (5) and (6). However T_γ only includes tangential stress due to streamline deflection. There will also be a frictional stress T_f along the screen proportional to the square of the velocity component parallel to the screen. From Fig. 3 it follows that the average absolute velocity across the screen for a flow passing at an angle γ to the normal is $u_0 \sin(\alpha + \gamma)$, and that the component of this absolute velocity along the screen is $u_0 \sin(\alpha + \gamma) \cos(\pi/2 - \gamma)$. Hence the total tangential force coefficient will be of the form $T_\gamma + T_f \sin^2(\alpha + \gamma) \cos^2(\pi/2 - \gamma)$. For the limit case $\gamma=0$ the flow passes normally through the screen, and there is no tangential velocity or frictional stress while T_γ attains its maximum value. For the other limit case $\gamma=(\pi/2 - \alpha)$ there is no deflection, hence $T_\gamma=0$ while the frictional stress coefficient becomes $T_f \cos^2(\alpha)$.

The drag force on the inclined screen can now be expressed by the pressure drop and tangential stress coefficients associated with u_0 as given below

$$F_D = \frac{1}{2} \rho u_0^2 A_{screen} \left(K \sin \alpha + (T_\gamma + T_f \sin^2(\alpha + \gamma) \cos^2(\pi/2 - \gamma)) \cos \alpha \right) \quad (11)$$

$$\begin{aligned} \frac{F_D}{(1/2)\rho u_0^2 A_0} &= K \sin \alpha \frac{A_{screen}}{A_0} + (T_\gamma + T_f \sin^2(\alpha + \gamma) \cos^2(\pi/2 - \gamma)) \cos \alpha \frac{A_{screen}}{A_0} \\ &= K + \frac{(T_\gamma + T_f \sin^2(\alpha + \gamma) \cos^2(\pi/2 - \gamma))}{\tan \alpha} \end{aligned} \quad (12)$$

For U the available coefficient from the literature is $C_N(K)$, e.g. as given by Eqs. (8) and (9), and represents the force normal to the screen. The tangential force coefficients associated with U must be included separately. For want of explicit coefficients we now argue that the each type of force must have the same value whether it is associated with U or u_0 , and that corresponding force coefficients can be related by the filtration efficiency F . By this is meant that although T_γ and T_f are basically associated with u_0 , they can also be associated with U if multiplied by F^2 . This also implies that we assume that filtration is governed by the pressure drop and that considering only K and C_N will also yield a reasonable approximation for F , cf. Eq. (16). However, for small angles of attack the tangential forces will be of greater relative importance both for the drag and the filtration, hence the tangential terms should be retained.

The drag force can now be expressed in terms of U as in Eq. (13), yielding Eq. (14) as an approximate model for the drag coefficient $C_D(K, T_\gamma, T_f, \dots)$ for the inclined screen. The corresponding lift coefficient for the screen is given by Eq. (15)

$$F_D = \frac{1}{2} \rho U^2 A_{screen} (C_N(K) \sin \alpha + F^2 (T_\gamma + T_f \sin^2(\alpha + \gamma) \cos^2(\pi/2 - \gamma)) \cos \alpha)$$

$$C_D = \frac{F_D}{(1/2) \rho U^2 A_0} \tag{13}$$

$$= C_N(K) \sin \alpha \frac{A_{screen}}{A_0} + F^2 (T_\gamma + T_f \sin^2(\alpha + \gamma) \cos^2(\pi/2 - \gamma)) \cos \alpha \frac{A_{screen}}{A_0}$$

$$= C_N(K) + \frac{F^2 (T_\gamma + T_f \sin^2(\alpha + \gamma) \cos^2(\pi/2 - \gamma))}{\tan \alpha} \tag{14}$$

$$C_L = \frac{F_L}{(1/2) \rho U^2 A_0} = \frac{C_N(K)}{\tan \alpha} - F^2 (T_\gamma + T_f \sin^2(\alpha + \gamma) \cos^2(\pi/2 - \gamma)) \tag{15}$$

Combining Eqs. (12) and (14) now yields the implicit relation Eq. (16) for the filtration efficiency of an inclined plane screen. Eq. (16) must be solved iteratively since K is a function of the actual Reynolds number at the screen and therefore depends on F . For the limit case $\alpha = 0^\circ$ we obtain $C_N(K) \rightarrow 0$ and $F \rightarrow 1$, and for $\alpha = 90^\circ$ we obtain $T_\gamma \cos \alpha \rightarrow 0$, $F \rightarrow \sqrt{C_N(K)}$ and $C_D = C_N$

$$F = \sqrt{\frac{u_0^2}{U^2}} = \sqrt{\frac{C_N(K) + F^2 (T_\gamma + T_f \sin^2(\alpha + \gamma) \cos^2(\pi/2 - \gamma)) / \tan \alpha}{K + (T_\gamma + T_f \sin^2(\alpha + \gamma) \cos^2(\pi/2 - \gamma)) / \tan \alpha}}$$

$$F_i = f \left(Re_{d,i-1} = \frac{(F_{i-1} U \sin \alpha) d}{\nu} \right) \tag{16}$$

5. Application of the model to conical nets

For a trawl or net section of general shape Eqs. (11)–(16) can be integrated over the net area to give the overall filtration and drag. For a circular net cone, however, axial symmetry and constant taper angle implies that Eqs. (14) and (16) describe the overall filtration and drag directly and that the lift force is zero, cf. Figs. 3 and 4. For K_0, K, T_γ, γ and C_N we use the expressions given by Eqs. (4)–(8). Løland’s model for C_N is chosen over Koo and James’ model because it is derived for two-dimensional flow and therefore suited for application to cones and trawls, recalling that Koo and James’ model is found to compare better with flow past three-dimensional plane screens (cf. Section 3). The value of T_f is difficult to specify with any accuracy. Wang and Matuda (1988, see O’Neill and O’Donoghue, 1997) find that $T_f = 0.02–0.04$ for diamond-meshed netting with low mesh opening angles, i.e. relatively low porosities. Although their results probably apply to coarser netting than typical plankton netting, and it is unclear if they also include tangential stress due to deflection, we assume that $T_f = 0.02$ is a reasonable choice for

the frictional stress coefficient. T_f is likely to increase with increasing roughness and decreasing Reynolds number, i.e. with increasing twine diameter and angle of incidence α (i.e. decreasing length of net) and decreasing velocity. Clogging and end effects, e.g. due to accumulated catch in the cod-end, are not considered here. The former may be accounted for by reducing the net area or as suggested for dirt build-up by Brundrett (1993), while the latter will have little influence on the upstream flow except in the vicinity of the catch in most cases.

The ratio between the open mesh area and mouth area of a circular net cone of constant taper ratio and porosity is $R_A = \beta / \sin \alpha$, cf. Eq. (10). Fig. 5 shows how the filtration efficiency varies with R_A and U according to Eq. (16), for a conical net with typical plankton mesh parameters. It shows that the common design recommendation for plankton net samplers cited in Section 2, i.e. that R_A should be greater than 3–6, is indeed reasonable and sufficient in many cases. However, the figure also shows that this approach may be misleading, e.g. when the Reynolds number is low.

6. Comparisons with measurements

In Figs. 6–15 Eqs. (14) and (16) are compared with measurements from Enerhaug (2005), who tests eight different

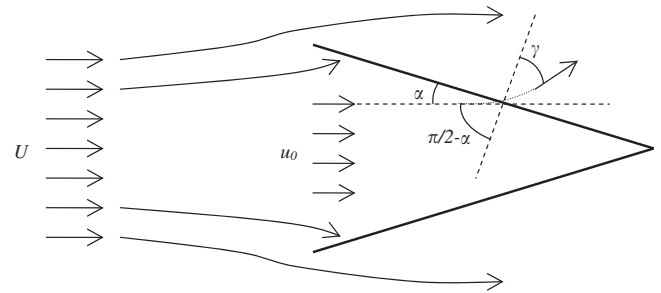


Fig. 4. Sketch of flow through and around a conical net.

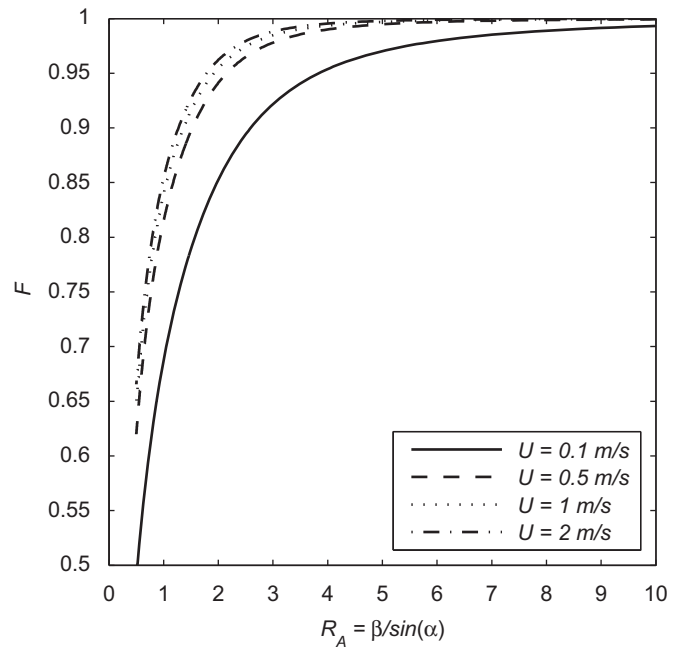


Fig. 5. Filtration efficiency F as a function of the “open-mesh-filtering-area to mouth area ratio” R_A for a square meshed conical net with $\beta = 0.5$, $d = 250 \mu\text{m}$ and $m = 600 \mu\text{m}$. F is calculated from Eq. (16) using K_0, K, T_γ, γ and C_N as given by Eqs. (4)–(8) and $T_f = 0.020$.

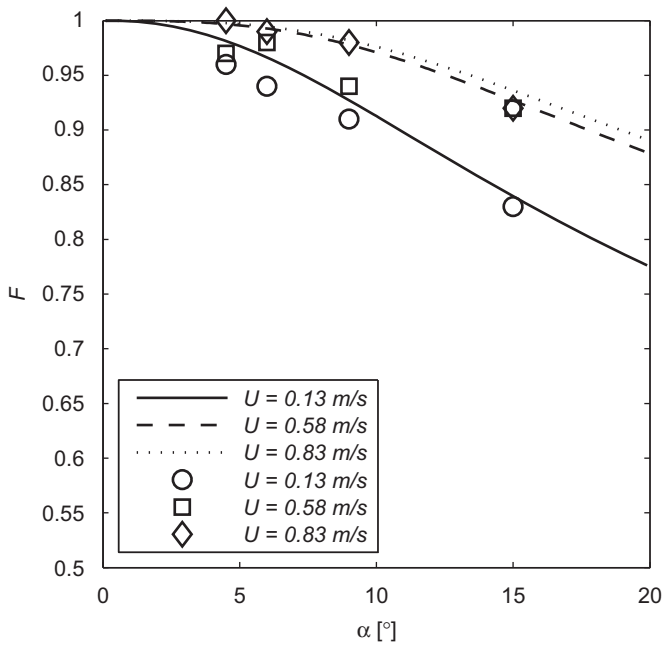


Fig. 6. F vs. α for $U=0.13, 0.58$ and 0.83 m/s. $\beta=0.47, d=230\ \mu\text{m}$ and $m=500\ \mu\text{m}$ for all cases. The lines represent Eq. (16) using K_0, K, T_p, γ and C_N as given by Eqs. (4)–(8) and $T_f=0.02$, while the markers represent measurements from Enerhaug (2005).

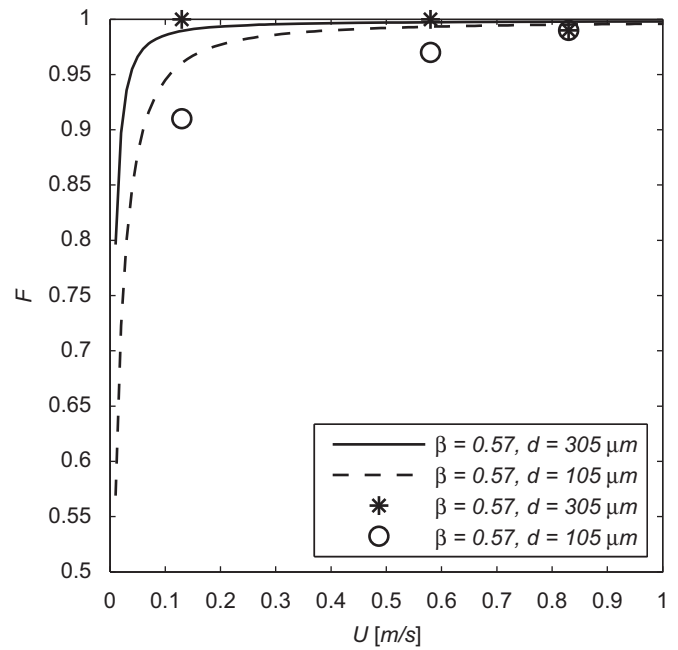


Fig. 8. F vs. U for two nets with $\alpha=6^\circ$, and with equal β but different d . The lines represent Eq. (16) using K_0, K, T_p, γ and C_N as given by Eqs. (4)–(8) and $T_f=0.02$, while the markers represent measurements from Enerhaug (2005).

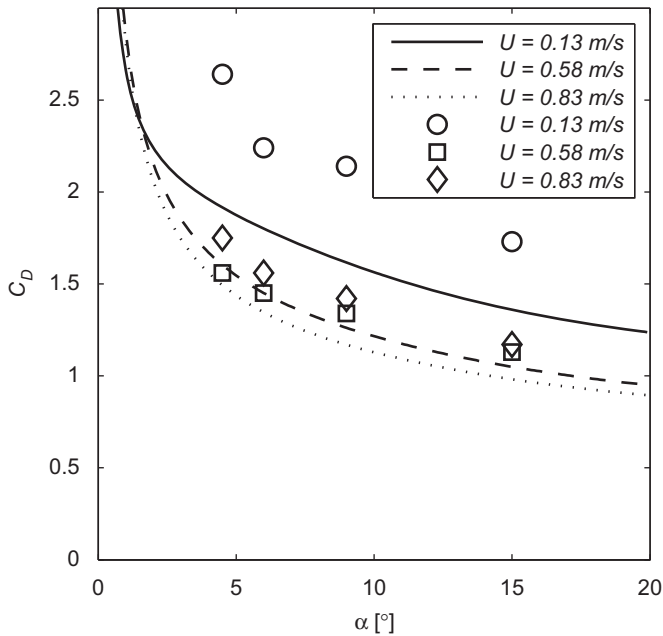


Fig. 7. C_D vs. α for $U=0.13, 0.58$ and 0.83 m/s. $\beta=0.47, d=230\ \mu\text{m}$ and $m=500\ \mu\text{m}$ for all cases. The lines represent Eq. (14) using K_0, K, T_p, γ and C_N as given by Eqs. (4)–(8) and $T_f=0.02$, while the markers represent measurements from Enerhaug (2005).

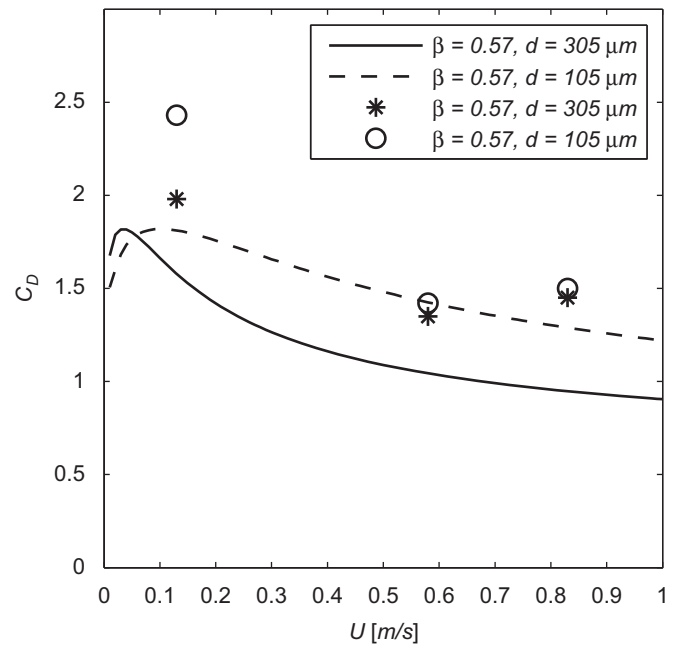


Fig. 9. C_D vs. U for two nets with $\alpha=6^\circ$, and with equal β but different d . The lines represent Eq. (14) using K_0, K, T_p, γ and C_N as given by Eqs. (4)–(8) and $T_f=0.02$, while the markers represent measurements from Enerhaug (2005).

nets at three current velocities $U=0.13, 0.58$ and 0.83 m/s in a flume tank 8 m wide, 2.7 m deep and 21.3 m long. The flume tank has a bottom conveyor belt running at the same speed as the nominal water velocity, hence avoiding a bottom boundary layer. The nets are made out of synthetic monofilament fabric with square mesh openings $143\ \mu\text{m} \leq m < 950\ \mu\text{m}$, twine thicknesses $105\ \mu\text{m} \leq d < 315\ \mu\text{m}$ and porosities $0.23\ \mu\text{m} \leq \beta < 0.57\ \mu\text{m}$. All nets have a mouth diameter of 0.8 m. The taper angle α varies from 4.5° to 15° , hence the lengths of the nets vary from 1.5 to

5.1 m. The nets are centred at a cross-section of the tank, with the net mouth at the same longitudinal position for all nets, and kept in place by a system of pre-tensioned lines. The circular front openings of the nets are ensured by stiff circular hoops 8 mm thick and 30 mm wide. Velocities are measured by a Höntzsch Vane Wheel at several locations at the cross-section of the net mouth, inside and outside the mouth, as well as at one position upstream of the net and at one position inside the net at 3/4 of the net length, both approximately at the centreline of the net. The

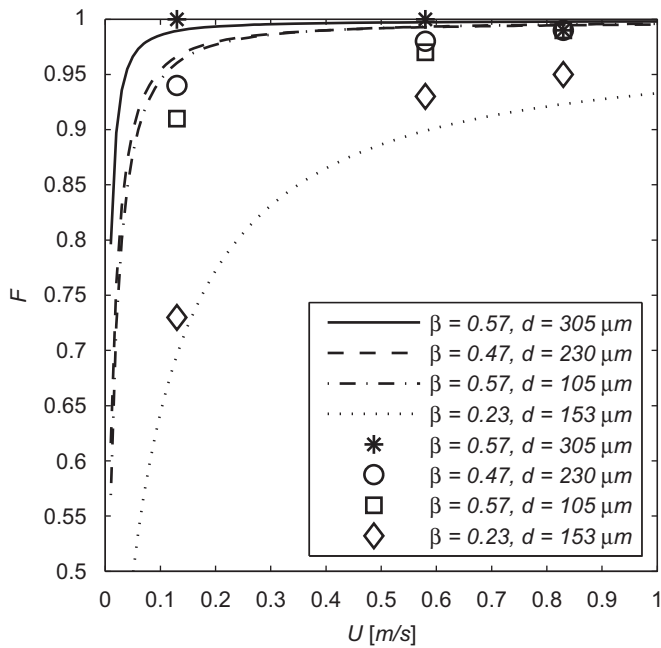


Fig. 10. F vs. U for four nets with $\alpha=6^\circ$, but with different β and d . The lines represent Eq. (16) using K_0 , K , T_p , γ and C_N as given by Eqs. (4)–(8) and $T_f=0.02$, while the markers represent measurements from Enerhaug (2005).

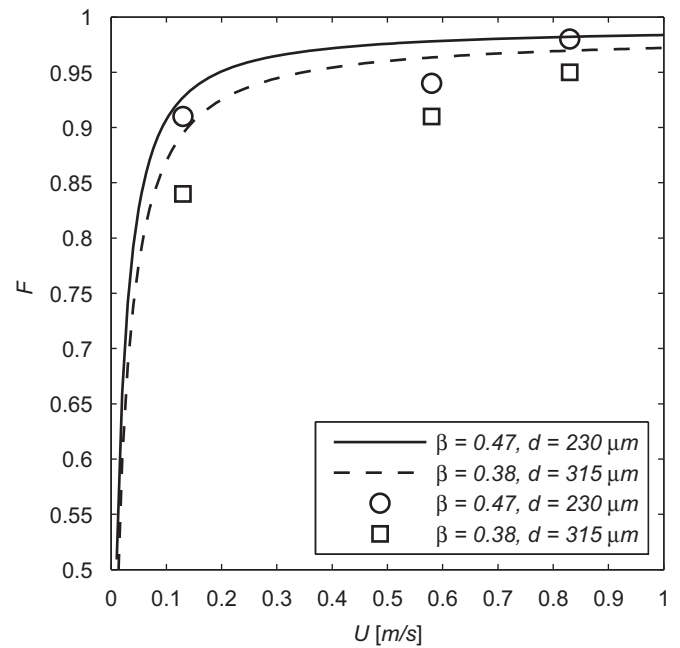


Fig. 12. F vs. U for two nets with $\alpha=9^\circ$, but with different β and d . The lines represent Eq. (16) using K_0 , K , T_p , γ and C_N as given by Eqs. (4)–(8) and $T_f=0.02$, while the markers represent measurements from Enerhaug (2005).

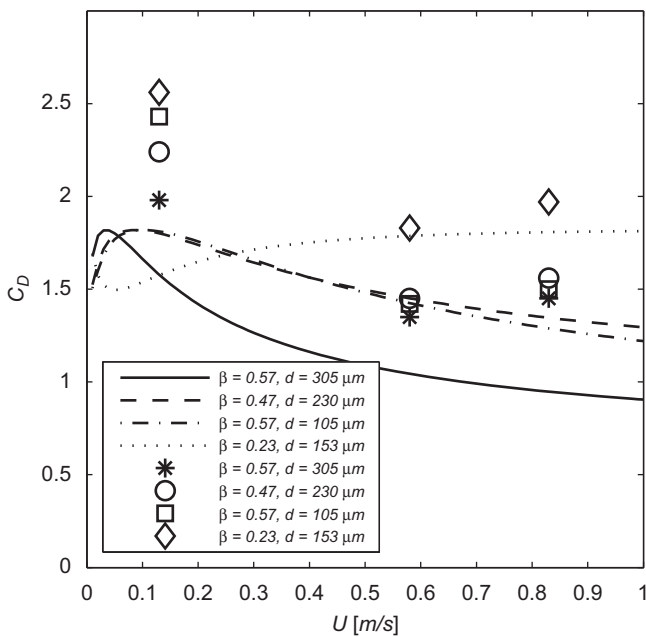


Fig. 11. C_D vs. U for four nets with $\alpha=6^\circ$, but with different β and d . The lines represent Eq. (14) using K_0 , K , T_p , γ and C_N as given by Eqs. (4)–(8) and $T_f=0.02$, while the markers represent measurements from Enerhaug (2005).

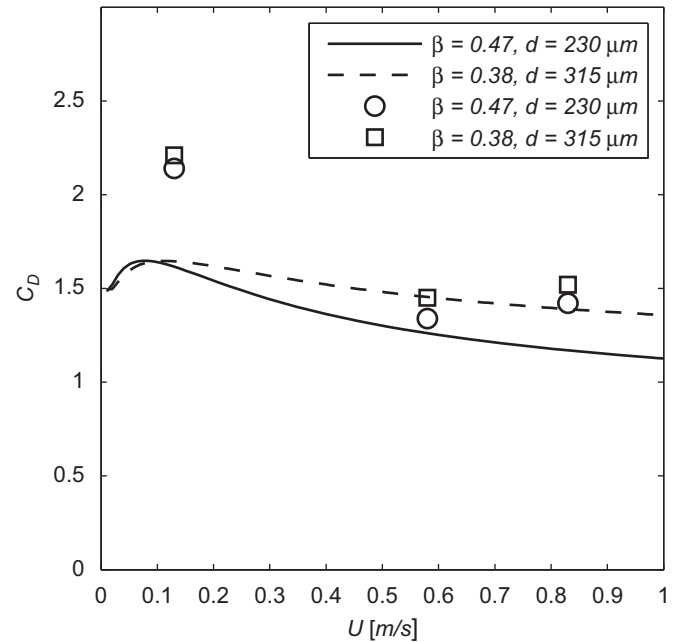


Fig. 13. C_D vs. U for two nets with $\alpha=9^\circ$, but with different β and d . The lines represent Eq. (14) using K_0 , K , T_p , γ and C_N as given by Eqs. (4)–(8) and $T_f=0.02$, while the markers represent measurements from Enerhaug (2005).

mouth velocity u_0 in Enerhaug (2005) is taken as the average of the measured velocity at three different positions at the cross-section of the mouth and a distance $\sqrt{2}/2 R$ from the centre of the mouth, i.e. as the average from three different positions along the dashed line in Fig. 1. The undisturbed velocity is taken as the average of the velocities measured at the exact same positions without any cone in the tank, hence assuming reproducibility rather than flow uniformity. Only the in-line (x) component of the velocity is measured. The drag is found from load cells in each line after subtracting the pre-tensioning in the lines.

Figs. 6 and 7 show how the filtration and drag vary with taper angle and velocity for four nets with equal mesh parameters but different taper angles. The parametric model compares well with the measurements, except for the filtration efficiency at the intermediate velocity $U=0.58$ m/s and the drag coefficient at the lowest velocity $U=0.13$ m/s. In the former case the measured filtration efficiencies vary in an apparently inconsistent manner, while in the latter case the measured drag coefficients are distinctly higher than the calculated ones. Qualitatively the calculated values behave reasonably. Figs. 8 and 9 show how

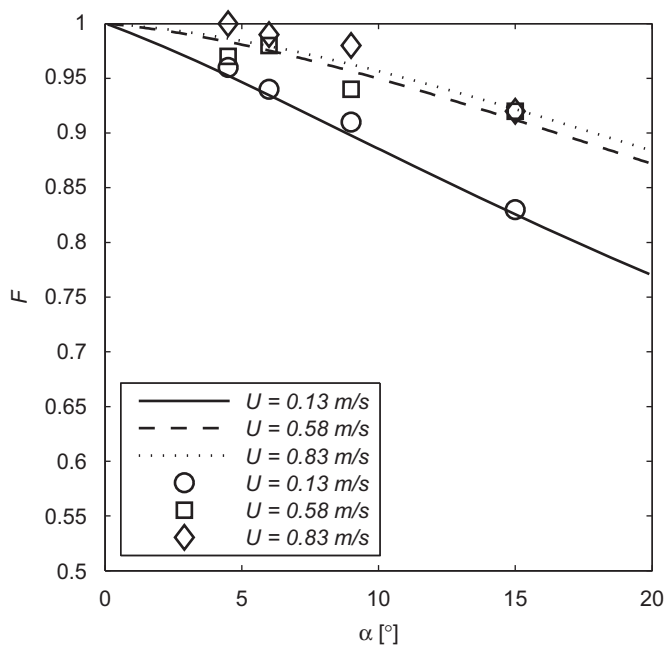


Fig. 14. F vs. α for the same cases as in Fig. 6 but ignoring the tangential forces in Eq. (16), i.e. $T_\gamma = T_f = 0$.

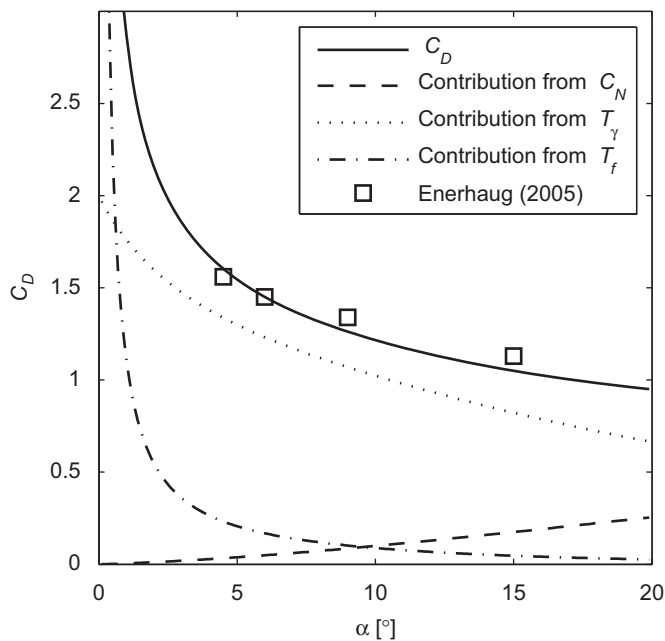


Fig. 15. C_D vs. α for the case $U=0.58$ in Fig. 7, showing the individual contributions to C_D due to C_N , T_γ and T_f , respectively.

the filtration and drag vary with velocity for two nets of equal porosity ($\beta=0.57$) and taper angle ($\alpha=6^\circ$) but with different twine thicknesses. The parametric model compares well with the measurements for the filtration. For the drag coefficient the model agrees well with the measured one for the thinner twine $d=105 \mu\text{m}$ at the two higher velocities, but underestimates it for the thicker twine. For the lowest velocity the drag coefficient is underestimated for both twine thicknesses. Figs. 10 and 11 show how the filtration and drag varies with velocity for four nets of equal taper angle ($\alpha=6^\circ$) but with different porosities and twine thicknesses. Again the comparison is quite good for the filtration, but with some discrepancy for the case $\beta=0.57$, $d=305 \mu\text{m}$. The

model also compares quite well with the measured drag coefficients at the two higher velocities, except for the net with $\beta=0.57$ and $d=305 \mu\text{m}$, for which it underestimates the drag coefficient. This is the same case as is underestimated in Fig. 9. Figs. 12 and 13 show how the filtration and drag vary with velocity for two nets of equal taper angle ($\alpha=9^\circ$) but with different porosities and twine thicknesses. The calculated filtration efficiencies are somewhat higher than the measurements, but qualitatively the comparison is good. The calculated drag coefficients compare quite well with the measured ones for the two higher velocities but are underestimated for the lowest velocity. Fig. 14 shows the same cases as Fig. 6, except that the tangential forces are neglected when calculating the filtration efficiency. It shows that the tangential terms have little influence on the filtration in this case, even though they constitute most of the total drag, cf. Fig. 15. The calculated filtration efficiency is slightly reduced when neglecting the tangential terms. Finally, Fig. 15 shows that the drag for these nets in this taper range is governed by the streamline deflection, except at low taper angles where friction becomes important. At higher taper angles C_N will dominate the drag.

It can also be noted that the drag measurements show a small but consistent increase in C_D as the velocity increases from $U=0.58$ to 0.83 m/s in Figs. 9, 11 and 13, while the parametric model predicts a slow decrease except for the low porosity case $\beta=0.23$ in Fig. 11. The drag measurements further show a distinct increase in C_D as the velocity decreases from $U=0.58$ to 0.13 m/s. The parametric model shows a similar behaviour, except for the low porosity case $\beta=0.23$ in Fig. 11, until $U \approx 0.1$ m/s where C_D drops off towards a value of about 1.5 as $U \rightarrow 0$.

7. Discussion

As cited in the introduction, Tranter and Heron (1967) state that “contrary to common belief” the filtration efficiency of both coarse and fine nets decreases with decreasing velocity. The blockage effect in trawls has for long been debated in the fisheries research community as well as among fishermen, and it is still a common perception that blockage generally increases as towing velocity increases. One likely reason for this is that while square-meshed plankton nets maintain their form and porosity well as the towing velocity and tension in the netting changes, other effects come into effect for more deformable (and common) mesh and net geometries. For instance, the porosity of a traditional diamond-meshed trawl section may decrease as towing velocity increases due to stretching and closure of meshes, in particular in cod-ends and extension pieces where the drag of the accumulated catch governs the net geometry (O’Neill and O’Donoghue, 1997). This may very well reduce the filtration efficiency in this part of the trawl. However, the global geometry and front opening of a traditional trawl may also change as towing velocity changes, so it is not straightforward to evaluate if changes in e.g. catch efficiency experienced by fishermen should be ascribed to a geometry change itself or to changed flow conditions due to the changed geometry. For plankton nets, clogging of the net walls may strongly influence filtration, and the clogging rate also varies with velocity. Fig. 5 shows that the design recommendations commonly used for plankton net samplers are indeed reasonable, but also that they may result in low filtration efficiency if used for very low Reynolds numbers and excessive drag, and in impractical design if used too conservatively.

The parametric model presented in this paper is compared with measurements of filtration and drag in Figs. 6–15. For the filtration the qualitative agreement is generally good while quantitatively the parametric model tends to overestimate

filtration in some cases. For the drag coefficient the comparison is also reasonable, but with three distinct discrepancies.

First, while the predicted drag coefficients compare well with the measured ones for $U=0.58$ and 0.83 m/s, except for the case $\beta=0.57$ and $d=305\ \mu\text{m}$ in Figs. 9 and 11, they are clearly lower than the measured ones for $U=0.13$ m/s. In the experiments the cones were pre-tensioned to maintain their form and orientation and to prevent dynamic variations during the test, and this tensioning force was then subtracted from the measurements. The pre-tensioning was equal for all three values of U . However, while the pre-tensioning was much less than the measured drag for $U=0.58$ and 0.83 m/s, it was higher than the measured drag for $U=0.13$ m/s. Hence the relative uncertainty in the measured values is considerably higher for $U=0.13$ m/s than for the other two velocities. Also, the drag due to the stiff hoop maintaining the front opening of the nets is not subtracted from the measured values, but it is estimated to constitute approximately 3% of the drag.

Second, the theoretical model predicts increasing drag coefficient with decreasing velocity, until the towing velocity drops below $U \approx 0.1$ m/s where C_D drops off towards a value of about 1.5 as $U \rightarrow 0$. This predicted drop occurs at lower velocities than were studied in the experiments. If the drag coefficient in reality increases consistently with decreasing towing velocity and at the rate suggested by the measurements, the drag coefficient at e.g. $U=0.01$ m/s will be quite high. However, as the towing velocity decreases the filtration also decreases and the flow will eventually resemble that past a solid cone, for which the drag coefficient is 1.2–1.4 for $Re_D > 10^4$ (Hoerner, 1965; White, 1988). Here Re_D is the Reynolds number for a solid cone based on mouth diameter and undisturbed flow velocity. Therefore the transition of C_D at low U towards a value comparable to that for a solid cone is indeed physically reasonable, also for the low porosity case $\beta=0.23$ in Fig. 11. An increase in the drag coefficient for a solid cone would not start to take place until Re_D drops below 10^4 , i.e. for $U < 0.0125$ m/s for a mouth diameter of 0.8 m. This latter effect is not included in the present model, nor are separation or global wake effects.

Third, the theoretical model appears to overestimate the effect of the Reynolds number on the drag coefficient for the case $\beta=0.57$ and $d=305\ \mu\text{m}$, cf. Figs. 9 and 11, i.e. it underestimates C_D in this case. One possible reason for this is that a thicker twine implies a higher roughness and tangential friction force, while the theoretical predictions are based on a constant friction coefficient $T_f \approx 0.020$. However, although this may explain some of the discrepancy, the tangential friction is relatively modest for $\alpha=6^\circ$ (cf. Fig. 15). The present authors believe that a more likely explanation can be found in the Gibbings's model (Gibbings, 1973) for the flow deflection γ , cf. Eqs. (6) and (7). This model has not previously been verified for $\alpha < 45^\circ$ and it seems plausible to assume that twine thickness may affect flow deflection and associated tangential force to a greater extent for small angles of incidence than accounted for in this model.

Also, the model predictions do not exhibit the small increase in C_D from $U=0.58$ to 0.83 m/s seen in the measurements in Enerhaug (2005), cf. Figs. 9, 11 and 13, except for in the low porosity case $\beta=0.23$ in Fig. 11. It remains unclear if this may be due to measurement uncertainties, since relatively small uncertainties in the measured velocity will lead to greater relative uncertainty in the normalized drag coefficient, global wake effects being neglected in the parametric model, or due to the limited accuracies in the simplified parametric model. Accuracy in all cases of course depends on the invoked models for K_0 , K , C_N , γ and T_f . The uncertainty in the model for γ seems to be of particular significance, considering its relative contribution to the total drag force, cf. Fig. 15.

Hence, some uncertainty remains regarding the drag coefficient predicted by the present model. For the filtration efficiency, however, the model performs well irrespective of the uncertainties for the drag coefficient. The reason for this is that the filtration is governed by the pressure drop, while the tangential forces only have a secondary effect on the filtration even if they may govern the total drag, cf. Eq. (16) and Figs. 14 and 15. This indicates that the pressure drop K and associated force $C_N(K)$ are well predicted by the model, and that the uncertainties for the drag coefficient are mainly related to the tangential forces. Consequently, and importantly, the filtration efficiency of an inclined screen or three-dimensional net cannot easily be derived from drag measurements alone.

8. Conclusions

This paper presents a parametric model for the flow through and forces on inclined permeable screens based on pressure drop considerations. For conical nets the model provides simple expressions for the filtration efficiency and drag as functions of twine diameter, mesh opening, porosity, taper angle and flow (towing) velocity.

Comparisons with experiments with fine-meshed plankton nets show good agreement between predicted and measured filtration efficiencies, demonstrating among other things how the filtration efficiency for a square-meshed conical net increases with increasing velocity and porosity and decreasing netting angle to the flow. The agreement between predicted and measured drag is also reasonable but not equally consistent, likely due to lack of sufficiently accurate models for flow deflection and tangential and frictional forces at low angles of attack. Since filtration is governed by the pressure drop and the tangential forces only have a secondary effect on filtration, there is no conflict between the results for the filtration efficiency and the drag. Another useful conclusion is thus that filtration efficiency cannot easily be derived from drag measurements alone.

Hence the theoretical model presented here provides a simple and reasonably accurate tool for predicting the filtration efficiency of plankton nets and trawls and how it varies with the towing velocity and net parameters. To get an equally reliable model for the drag force it seems necessary to develop improved models for flow deflection and friction coefficients, especially for low angles of attack.

Acknowledgements

This work was funded by The Research Council of Norway through the Fisheries Technology Programme Project No. 153140.

References

- Brundrett, E., 1993. Prediction of pressure drop for incompressible flow through screens. *Journal of Fluids Engineering* 115, 239–242.
- Carrothers, P.J.G., Baines, W.D., 1975. Forces on screens inclined to a flow. *Journal of Fluids Engineering* 97, 116–117.
- Enerhaug, B., 2005. Flow through fine-meshed pelagic trawls. In: Lee, C.-W. (Ed.), *Contributions on the Theory of Fishing Gears and Related Marine Systems*, vol. 4 (Proceedings of the DEMaT '05), Busan, Korea, November 23–26, 2005, pp. 153–164.
- Ferro, R.S.T., Van Marlen, B., Hansen, K.E., 1996. An empirical velocity scale relation for modelling a design of large mesh pelagic trawl. *Fisheries Research* 28, 197–230.
- Fredheim, A., 2005. Current forces on net structures. Doctoral Thesis, Department of Marine Technology, Norwegian University of Science and Technology, ISBN 82-471-6999-1/82-471-6998-3 (electronic version).

- Fridman, A.L., Carrothers, P.J.G. (Eds.), 1986. Calculations for Fishing Gear Design. Fishing News Books.
- Gibbins, J.C., 1973. The pyramid gauze diffuser. *Ingenieur-Archiv* 42, 225–233.
- Graham, J.M.R., 1976. Turbulent flow past a porous plate. *Journal of Fluid Mechanics* 73 (3), 565–591.
- Groth, J., Johansson, A.V., 1988. Turbulence reduction by screens. *Journal of Fluid Mechanics* 197, 139–155.
- Harris, R.P., Wiebe, P.H., Lenz, J., Skjoldal, H.R., Huntley, M. (Eds.), 2000. ICES Zooplankton Methodology Manual. Academic Press.
- Hoerner, S.F., 1952. Aerodynamic properties of screens and fabrics. *Textile Research Journal* 22, 274–280.
- Hoerner, S.F., 1965. Fluid-dynamic Drag. Hoerner Fluid Dynamics.
- Hu, F., Matuda, K., Tokai, T., 1999. Similarity laws and modelling rules for fishing nets. In: Paschen, M., Köpnick, W., Niedzwiedz, G., Richter, U., Winkel, H.-J. (Eds.), Contributions on the Theory of Fishing Gears and Related Marine Systems (Proceedings of the DEMaT '99). University of Rostock.
- Koo, J.-K., James, D.F., 1973. Fluid flow around and through a screen. *Journal of Fluid Mechanics* 60 (Part 3), 513–538.
- Koritzky, H.H., 1974. Beitrag zur Bestimmung von Widerstand und Auftrieb ebener Netztücher. Doctoral Thesis, University of Rostock.
- Laws, E.M., Livesey, J.L., 1978. Flow through screens. *Annual Review of Fluid Mechanics* 10, 247–266.
- Løland, G., 1991. Current forces on and flow through fish farms. Doctoral Thesis, Department of Marine Hydrodynamics, The Norwegian Institute of Technology.
- Løland, G., 1993. Water flow through and around net pens. In: Proceedings of the First International Conference on Fish Farming Technology, Trondheim, August 9–12, 1993, pp. 177–183.
- O'Neill, F.G., 1993. Small-scale modelling rules of trawl nets. *Fisheries Research* 18, 173–185.
- O'Neill, F.G., O'Donoghue, T., 1997. The fluid dynamic loading on catch and the geometry of trawl cod-ends. *Proceedings of the Royal Society of London A* 453, 1631–1648.
- O'Neill, F.G., 2006. Source models of flow through and around screens and gauzes. *Ocean Engineering* 33, 1884–1895.
- Paschen, M., Winkel, H.J., 1999. Flow investigations of net cones. In: Paschen, M., Köpnick, W., Niedzwiedz, G., Richter, U., Winkel, H.-J. (Eds.), Contributions on the Theory of Fishing Gears and Related Marine Systems. (Proceedings of the DEMaT '99). University of Rostock.
- Reynolds, A.J., 1969. Flow deflection by gauze screens. *Journal of Mechanical Engineering Science* 11, 290–294.
- Schubauer, G.B., Spangenberg, W.G., and Klebanoff, P.S., 1950. Aerodynamic characteristics of damping screens. NACA Technical Note No. 2001.
- Smith, P.E., Counts, R.C., Clutter, R.I., 1968. Changes in filtering efficiency of plankton nets due to clogging under tow. *Journal du Conseil/Conseil International pour l'Exploration de la Mer* 32, 232–248.
- Taylor, G.I., 1944. Air resistance of a flat plate of very porous material. *Aeronautical Research Council Reports and Memoranda* No. 2236.
- Taylor, G.I., Davies, R.M., 1944. The Aerodynamics of porous sheets. *Aeronautical Research Council Reports and Memoranda* No. 2237.
- Taylor, G.I., Batchelor, G.K., 1949. The effect of wire gauzes on small disturbances in a uniform stream. *Quarterly Journal of Mechanics and Applied Mathematics* 2, 1–29.
- Tranter, D.J., 1967. A formula for the filtration coefficient of a plankton net. *Australian Journal of Marine and Freshwater Research* 18, 113–121.
- Tranter, D.J., Heron, A.C., 1967. Experiments on filtration in plankton nets. *Australian Journal of Marine and Freshwater Research* 16, 281–291.
- Tranter, D.J., Smith, P.E., 1968. Filtration performance. *Zooplankton Sampling: Monographs on Oceanographic Methodology*, vol. 2. UNESCO.
- Wakeland, R.S., Keolian, R.M., 2003. Measurements of resistance of individual square-mesh screens to oscillating flow at low and intermediate Reynolds numbers. *Journal of Fluids Engineering* 125, 851–862.
- Ward, J.N., Ferro, R.S.T., 1993. A comparison of one-tenth and full-scale measurements of the drag and geometry of a pelagic trawl. *Fisheries Research* 17, 311–331.
- White, F.M., 1988. *Fluid Mechanics*, 2nd ed McGraw-Hill.
- Wiebe, P.H., Benfield, M.C., 2003. From the Hensen Net toward four-dimensional biological oceanography. *Progress in Oceanography* 56 (1), 7–136.
- Wiegardt, K.E.G., 1953. On the resistance of screens. *Aeronautical Quarterly* 4, 186–192.